An Innovative Magnetic Density Separation Process

Lin Wang *, Peter Rem, Francesco Di Maio *, Max Van Beek, Gonçalo Tomás

Posted Date: 19 March 2024

doi: 10.20944/preprints202403.1063.v1

Keywords: magnetic density separation; magnetic fluid; granular sorting; particle sliding phenomenon; solid waste; wasted PCBAs; wasted wires

Article

An Innovative Magnetic Density Separation Process

Lin Wang [1,*], Peter Rem [1], Francesco Di Maio [1,*], Max van Beek [1] and Gonçalo Tomás [2]

[1] Resource & Recycling, Department of Engineering Structures, Faculty of Civil Engineering and Geosciences, Delft University of Technology, Delft, The Netherlands; l.wang-13@tudelft.nl (L.W.); p.c.rem@tudelft.nl (P.R); f.dimaio@tudelft.nl (F.D.M.); m.c.vanbeek@tudelft.nl (M.V.B)

[2] Faculty of Science and Technology, University of Twente, Enschede, The Netherlands; g.s.santostomas@utwente.nl

* Correspondence: l.wang-13@tudelft.nl (L.W.); f.dimaio@tudelft.nl (F.D.M.)

Abstract: Motivated by the PEACOC project on metal recovery from solid wastes, an innovative magnetic density separation (MDS) process has been developed for granular material sorting. It has intrinsic advantages over the existing industrialized MDS by eliminating fluid turbulence and particle jamming problems. The new MDS applies an inclined planar magnet and a horizontal basin containing a static magnetic fluid as the separation medium. A particle sliding phenomenon is identified as a feature of the process which could help the separation. The MDS successfully sorted shredded PCBAs to concentrate valuable metals and sorted shredded wires to reduce metallic contaminants in the plastic fractions. A pilot scale facility is introduced to show the design to achieve continuous production and to reduce the consumption of ferrofluid.

Keywords: magnetic density separation; magnetic fluid; granular sorting; particle sliding phenomenon; solid waste; wasted PCBAs; wasted wires

1. Introduction

Magnetic density separation (MDS) is a process to separate non-magnetic solid particles by their densities. It applies a magnetic fluid under a gradient magnetic field as the separation medium. Magnetic fluid was invented in 1960s as a liquid colloid composed of a base liquid and suspended magnetic nanoparticles so that it can be attracted by a magnet [1,2]. Later it was found that the downward magnetic attraction on a magnetic fluid exerted by a magnet beneath the fluid resulted in an upward fluidmagnetic buoyancy on a non-magnetic particle in the fluid [3]. As a result, the particle with its density higher than the fluid density could float rather than sink. The fluidmagnetic buoyancy would continuously increase as the particle in the fluid moves downward, i.e. closer to the magnet. Therefore, the particle dropped in the fluid may neither sink to the bottom nor float at the fluid surface, but suspend at a certain height where its gravity equals the sum of fluidmagnetic buoyancy and the original buoyancy without magnetic field. This allows the separation between particles with different densities since they would suspend at different heights. The separation is called MDS and has been studied in the past decades [4–6] across a wide range of applications including resource recovery (car metals [7]; incinerator bottom ash [8,9]; WEEE [10]; plastics [11–14]), mineral processing (coal preparation [15]; diamond and precious metal enrichment [16–18]), and seed sorting [19].

The MDS could be economically promising in solid waste sorting for resource recovery [20]. With the innovative planar magnet [21] and synthesis method of magnetic fluid [22,23], Peter Rem et al. successfully industrialized the MDS for plastic sorting with a certain design of separation channel which facilities are being used by Umincorp in the Netherlands [24,25]. In the separation channel [26], a magnetic fluid is continuously flowing horizontally and transporting fed particles through a laminator, a separation zone, and a collection zone in sequence. The laminator creates a laminar fluid flow for the separation zone. The separation zone is under a gradient magnetic field, thus heavier particles form lower streams and lighter particles form higher streams. Splitters are used in the

 doi:10.20944/preprints202403.1063.v1

collection zone to split separated particle streams at different heights for collection. The throughput of this system depends on the fluid flow velocity because the particles are conveyed by the fluid, but increasing the fluid velocity could cause more turbulence that may affect the separation accuracy in the separation zone. Corresponding studies were carried out to examine the turbulence effect [26–28] and suggested to carefully design the structure and control the fluid velocity. In addition, if a particle entering the splitter zone has a dimension larger than the distance between two splitter walls (e.g. 2 cm), it may get stuck and block subsequent particles. Based on the above knowledge, this work introduces a different innovative MDS process with corresponding advantages. Firstly, the new process applies a static magnetic fluid rather than flowing fluid, thus the process is no longer affected by turbulence. Secondly, no splitters are used in the new process, thus the process is no longer affected by particle jamming. The development of the MDS was motivated by the PEACOC project of European Union aiming for metal recovery from solid wastes. This work will firstly introduce the principle of the new MDS process, illustrating how particles are driven in the magnetic fluid and how they are split without splitters. Then a particle sliding phenomenon will be introduced and demonstrated experimentally and numerically. Since the new process was developed as an advanced granular sorting technology to contribute to solid waste sorting, experiments on sorting shredded PCBAs and sorting shredded wires will be shown and discussed. Lastly, a pilot scale facility will be introduced to illustrate how to realize a continuous and economic industrial process.

2. Materials and Methods

2.1. Principle of the Innovative MDS

Figure 1 shows the principle of the new MDS process, where particle motion was simulated using LIGGGHTS [29]. The forces on one specific particle are also shown in the figure (the fluid drag force on the particle is not shown but was calculated in the simulation). The process applies a tilted magnet with a planar upper surface. The magnet can be either a permanent magnet [21] comprising an array of pole pieces or a super-conducting electromagnet [30,31] comprising an array of coils. This work applies a permanent magnet. The field strength above the magnet decreases exponentially with the normal distance to the magnet [14]:

$$|\boldsymbol{B}| = B_0 e^{-\pi z/p} \tag{1}$$

where B_0 is the field strength magnitude at the magnet surface, p is the pole size of the magnet, and z is the normal distance to the magnet. A basin with a horizontal bottom containing magnetic fluid is placed above the magnet. The fluidmagnetic buoyancy $\boldsymbol{F}_{mag\_buoyancy}$ on the particle immersed in the fluid has the same magnitude but opposite direction as the magnetic attraction exerted by the magnet on the fluid displaced by the particle [14]:

$$\left|\boldsymbol{F}_{mag\_buoyancy}\right| = MV_p \frac{\pi B_0}{p} e^{-\pi z/p} \tag{2}$$

where M is the magnetization of the fluid and V_p is the volume of the particle. The gradient of the magnetic field is perpendicular to the magnet, so the particles with different densities dropped in the fluid would find their respective equilibrium positions along the normal direction to the magnet. The inclination of the magnet results in a horizontal component of $\boldsymbol{F}_{mag\_buoyancy}$ on the particle which drives the particle forward (to the right side). Therefore, particles move both downward and forward along trajectories parallel to the magnet, then deposit on the basin bottom. The trajectories of heavier particles are closer to the magnet, while lighter particles are higher so they move further before depositing on the basin bottom. Therefore, particles with different densities are distributed at different positions on the bottom. In practice, the deposited particles can be conveyed by a horizontal belt to be collected. The belt should lie on the basin bottom moving along the perpendicular direction to the plane of Figure 1.

 doi:10.20944/preprints202403.1063.v1

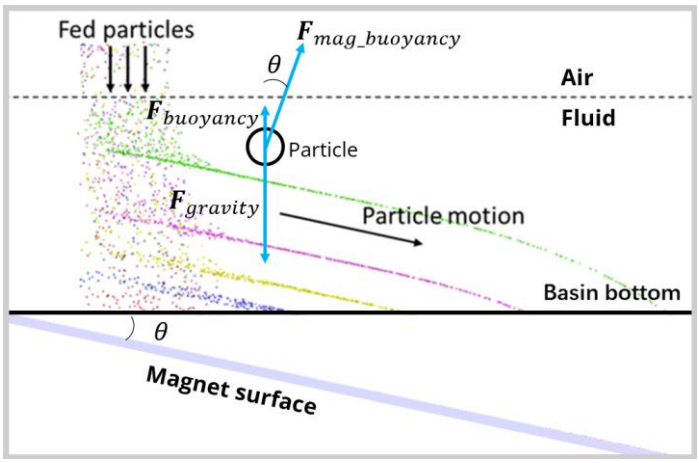

Figure 1. Principle of the innovative MDS.

2.2. Particle Sliding Phenomenon

A particle sliding phenomenon was identified as a feature of the above MDS process. When a particle moving in the fluid along its inclined trajectory reaches the horizontal bottom of the basin, it would slide forward rather than immediately stop. The phenomenon was demonstrated both experimentally and numerically.

2.2.1. Experimental Demonstration

Figure 2(a) shows the experimental setup for the demonstration. A transparent container containing some black ferrofluid (magnetic fluid produced by Umincorp in the Netherlands) was placed horizontally above the inclined permanent magnet. It is notable that the fluid surface on the left was higher than the right, because the left part of the fluid was closer to the magnet thus was attracted more. Figure 2(a) also shows two particles to be dropped in the fluid. Particle 1 was brass and Particle 2 was aluminium. Some physical parameters related to the experiment are listed in Table 1.

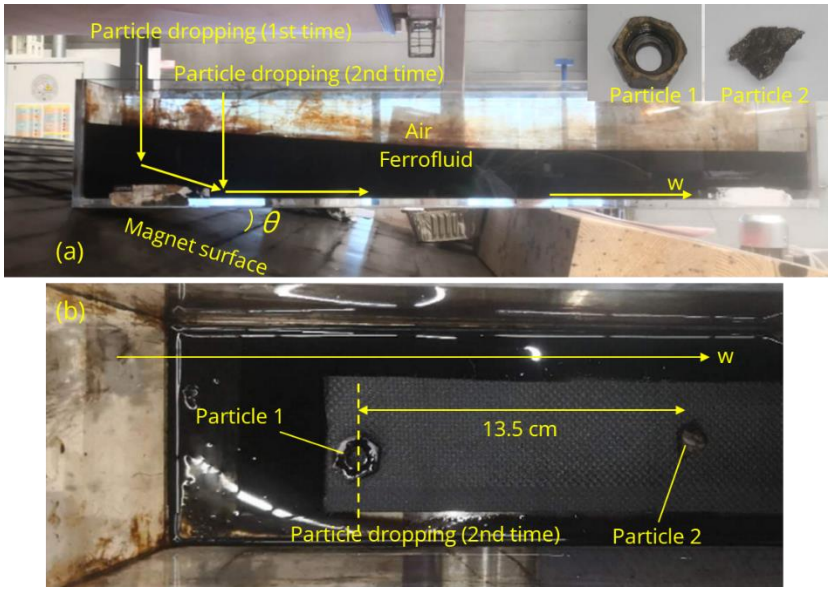

Figure 2. (a) Experimental setup to demonstrate particle sliding; (b) top view of deposited particles.

 doi:10.20944/preprints202403.1063.v1

Table 1. Physical parameters.

Parameter	Value
Density of Particle 1, ρ_{p1}	8500 kg/m^3
Density of Particle 2, ρ_p	2700 kg/m^3
Particle volume, V_p	1 cm^3
Angle of magnet surface to basin bottom, θ	12°
Fluid density, ρ	1032 kg/m^3
Fluid magnetization, M	3368 A/m
Magnetic field strength at magnet surface, B_0	0.63 T
Magnet pole size, p	0.189 m

Particle 2 was firstly dropped in the fluid from the left, corresponding to 'Particle dropping (1st time)' in Figure 2(a). The estimated dropping position on the w axis was close to the left edge of the container so that Particle 2 firstly moved downward then followed the inclined trajectory until it reached the bottom. Note that if Particle 1 was dropped from the same position, it would not have the inclined trajectory but directly sink to the bottom, because its density was too high considering the given magnetic field strength and fluid magnetization. It could not be levitated by the fluid even if it was at the left bottom corner of the container where the fluidmagnetic buoyancy was the largest. The position on the w axis where Particle 2 first touched the bottom could not be directly observed. Because the fluid is so black that any particle in it is not visible. To obtain the position, a board was put in the fluid to stop Particle 2 on its path. The board surface was perpendicular to the inclined particle trajectory. After Particle 2 was stopped by the board, the fluid was slowly pumped out until Particle 2 appeared at the fluid surface, then its position could be marked. By changing the position of the board on the w axis several times and repeating dropping Particle 2 and marking its position, the inclined trajectory of Particle 2 was marked and the position where it first touched the bottom was known. The position was then used as the position of the second dropping, corresponding to 'Particle dropping (2nd time)' in Figure 2(a). In the second dropping both Particle 1 and Particle 2 were dropped. The role of Particle 1 was to mark the dropping position as the dash line shows in Figure 2(b). Figure 2(b) shows the final positions of the particles on the bottom after the second dropping and after the fluid was pumped out. Particle 2 was found to slide across 13.5 cm after it reached the bottom. It is interesting that in the first dropping, the sliding distance of Particle 2 was also 13.5 cm. This indicates that the velocity of Particle 2 along $+w$ when it first touched the bottom contributed very little to its sliding distance on the bottom.

2.2.2. Numerical Demonstration

The reason that Particle 2 was driven to slide on the bottom is numerically illustrated. Figure 3(a) shows the forces on Particle 2 sliding on the bottom. The orange dash arrow lines mark its trajectory. On the w axis, when the particle was at $w = w_1$, the net force along the normal direction to the magnet was zero:

$$\left|\boldsymbol{F}_{gravity}\right| \cos\theta = \left|\boldsymbol{F}_{buoyancy}\right| \cos\theta + \left|\boldsymbol{F}_{mag\_buoyancy}\right| \tag{3}$$

which is:

$$\rho_p g V_p \cos\theta = \rho g V_p \cos\theta + M V_p \frac{\pi B_0}{p} e^{-\pi z/p} \tag{4}$$

where $z = w_1 \sin\theta$. With the parameters in Table 1, w_1 can be calculated as 23 cm. When Particle 2 is sliding on the bottom, i.e. $w = w_1 + w_2$, the vertical net force on the particle is zero:

$$\left|\boldsymbol{F}_{buoyancy}\right| + \left|\boldsymbol{F}_{normal}\right| + \left|\boldsymbol{F}_{mag\_buoyancy}\right| \cos\theta = \left|\boldsymbol{F}_{gravity}\right| \tag{5}$$

Note that $z = (w_1 + w_2)\sin\theta$. Assuming the sliding friction coefficient μ is 0.5, the sliding friction $\left|\boldsymbol{F}_{sliding}\right| = \mu\left|\boldsymbol{F}_{normal}\right|$ can be calculated with a given w_2. Figure 3(b) shows the variations of $\left|\boldsymbol{F}_{sliding}\right|$ and the horizontal component of $\left|\boldsymbol{F}_{mag\_buoyancy}\right|$ with w_2. When $w_2 = 0$, $\left|\boldsymbol{F}_{sliding}\right|$ was

Preprints.org (www.preprints.org) | NOT PEER-REVIEWED | Posted: 19 March 2024 doi:10.20944/preprints202403.1063.v1

much smaller than $|\boldsymbol{F}_{mag\_buoyancy}| \sin\theta$. This indicates that Particle 2 was being accelerated along $+w$ when it first touched the bottom, demonstrating the inevitability of the particle sliding phenomenon. In the case of Figure 3(b), only after Particle 2 slides to w_2 = 0.09 m, it starts to slow down.

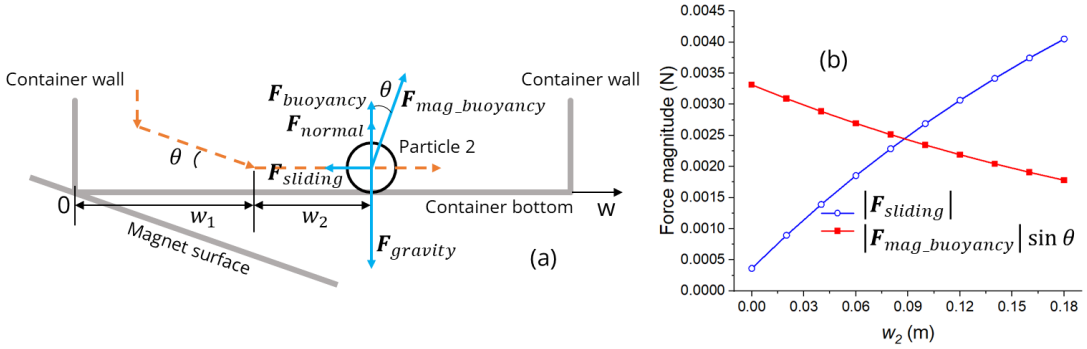

Figure 3. (a) Forces on Particle 2 on the bottom; (b) variation of horizontal forces with w_2.

The particle sliding phenomenon suggests a useful technique to improve the separation performance. For example, in the case of Figure 2(b), if Particle 2 did not slide on the bottom, it would have the same final position with Particle 1 on the bottom. That means separation between them was not possible unless the fluid magnetization or the magnetic field strength was increased. However, with the particle sliding phenomenon, Particle 2 was 13.5 cm further than Particle 1 on the bottom. That distance was large enough for distinguishing two particle streams and separately collecting them.

2.3. MDS Experiments on Material Sorting

To demonstrate the effectiveness of the above MDS process in solid waste sorting, experiments were carried out to sort shredded PCBAs to concentrate valuable metals, and sort shredded wires to purify plastic fractions. Figure 4(a) shows the experimental setup. A transparent rectangular container was placed horizontally above the inclined magnet and was filled with ferrofluid using a pump. The magnet had a rectangular upper surface of 1.2 m × 1.15 m and its other physical parameters matched Table 1. The magnetization of the fluid was 2000 A/m. In the experiment, the feedstock scraps were dropped into the fluid close to the left edge of the container. The dropped scraps then moved in the fluid and deposited at different positions along the w axis on the bottom of the container. Scraps with higher densities were closer to the left side, while lighter scraps were further to the right.

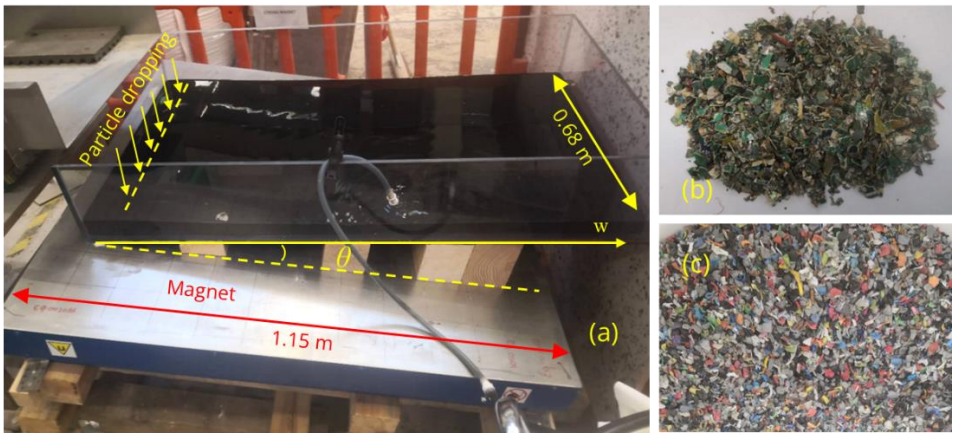

Figure 4. (a) Experimental setup for material sorting; (b) feedstock of shredded PCBAs; (c) feedstock of shredded wires.

 doi:10.20944/preprints202403.1063.v1

Figure 4(b) shows the feedstock of shredded PCBAs. It was the fraction after removing foil scraps by wind sifting and removing magnetic scraps by magnetic sorting from the original shredded PCBAs. Note that the magnetic scraps are also rich in valuable metals. However, magnetic particles are not the proper feedstock to be separated by MDS since they would always be attracted to the bottom by the magnet once dropped in the fluid. This work focused on the effectiveness of MDS in material sorting thus the magnetic scraps are not discussed here. The feedstock in the MDS was 77.2 wt% of the original shredded PCBAs. The original shredded PCBAs were provided by TREEE in Italy, a partner within the PEACOC project. The PCBAs were from CRT-TVs and monitors and were shredded to below 1.8 cm.

Figure 4(c) shows the feedstock of shredded wires. It was the plastic fraction separated from original shredded wires by air table sorting in cable recycling industries in the Netherlands. Before the air table sorting, the wires were shredded to 1-8 mm long pieces when most copper wires were liberated from the plastic hulls. The copper wires were then separated from the plastics by air blowing the particles vibrated on a tilted table. The feedstock was provided by Myne in the Netherlands.

3. Results and Discussion

3.1. MDS Sorting of Shredded PCBAs

The innovative MDS was developed to contribute to the PEACOC project aiming for metal recovery from solid wastes. Wasted PCBAs is one of the main wastes to be processed. The amount of wasted PCBAs has been increasing fast in most countries which is a hazard to the environment. The waste is also a source of multiple valuable metals. The recycling is complicated especially when it is required to be environmental-friendly and profitable [32]. In this experiment, the sorting of shredded PCBAs was to concentrate valuable metals such as gold, silver, and copper. It was speculated that the valuable metals mainly existed in heavier scraps. Like mineral processing, the MDS could sort the feedstock into a rich fraction and a poor fraction, thus the cost to process the poor fraction could be saved.

After dropping the feedstock of shredded PCBAs in the fluid as shown by Figure 4(a), the fluid was pumped out and the top view of deposited particles on the bottom is shown in Figure 5. Along the w axis, the particles were manually divided into three streams. XRF and lead assay analyses were carried out to obtain the mass fractions of gold, silver, and copper in each of the three streams, as well as in the original shredded PCBAs and the feedstock in the MDS. The results are shown in Table 2 where the mass of each particle stream is also listed. Compared with the original shredded PCBAs, the metals in the MDS feedstock were already concentrated a little. After the MDS, the metals in Stream 1 and Stream 2 were concentrated, while Stream 3 with a considerable amount was a poor stream. It indicates that the metals mainly exist in heavier scraps that were distributed on the left of the container. On the right of the container the scraps were lighter and visibly less-metallic which mainly consist resins and plastics. Stream 1 and Stream 2 can be collected as the concentrate product and Stream 3 can be regarded as the tailing. Compared with the MDS feedstock, the mass contents of Au, siler and Cu in the concentrate product were increased by 71.3%, 60.6% and 142.7% respectively, and the recovery rate was 99.94%, 93.74% and 100% correspondingly. It demonstrates that the MDS could be effective in the concentration of Au, Ag and Cu in the shredded PCBAs. Note that the tailing Stream 3 was 41.7 wt% of the MDS feedstock. Considering the density of Stream 3 was much smaller than Stream 1 and Stream 2, the bulk volume fraction of Stream 3 was even larger. Therefore, removing Stream 3 by the MDS sorting could save much cost to process the material in subsequent metallurgical processes.

 doi:10.20944/preprints202403.1063.v1

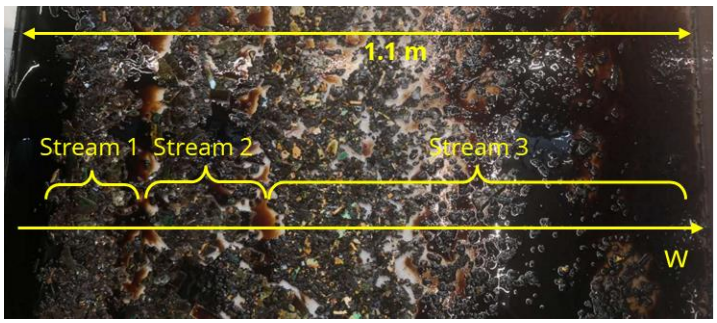

Figure 5. Top view of deposited PCBA scraps.

Table 2. Mass of each particle stream and mass contents of Au, Ag and Cu in each stream.

Particle stream	Mass	Au content	Ag content	Cu content
Original shredded PCBAs	9683.9 g	18.56 ppm	612.73 ppm	9.55%
MDS feedstock	7479.9 g	20.30 ppm	682.89 ppm	10.24%
Stream 1	2654.5 g	30.07 ppm	1369.33 ppm	29.57%
Stream 2	1710.3 g	42.05 ppm	674.35 ppm	17.53%
Stream 3	3115.4 g	0.03 ppm	102.63 ppm	0.00%

3.2. MDS Sorting of Shredded Wires

The role of the new MDS in the recycling of wasted electrical wires was also demonstrated. The traditional recycling of wasted cables focused on copper recovery. However, the plastic fraction is a hazard to the environment especially when it goes to landfill or incineration. That is why the proper recycling of the plastic fraction is also important [33,34]. Economic recycling of the plastics requires techniques to purify the plastic fractions separated from metal fractions. In this experiment, the MDS feedstock which was the plastic fraction after air table sorting still contained a small amount of copper. It could be copper wires, non-liberated copper wires covered by plastic hulls, or small copper particles generated during shredding. The impurity of the plastic fraction increases the cost of plastic reproduction, and it is also a waste of copper.

Using the same MDS setup as Figure 4(a), the wire scraps deposited on the container bottom as shown in Figure 6. Note that before the MDS, the float was removed using water. Along the w axis, the particles were manually split into six streams. XRF analysis was carried out for each stream, as well as the feedstock and the float. Copper and Aluminium were found to be the main metallic contaminants in the feedstock. Different from copper which existed in the form of conductive wires, aluminium wires were not observed, thus it is speculated that aluminium existed as a component of the sheathing material. Table 3 shows the Cu and Al contents in each particle stream and the mass of each particle stream. In Stream 3, 5, 6 and the float, the metallic contaminants were obviously reduced compared with the feedstock. Considering the feedstock was already the separated plastic fraction from the original shredded wires, the MDS could be an advanced alternative to the air table sorting applied by cable recycling industries in the Netherlands. The MDS also has the unique advantage to separate the feedstock into multiple streams with different densities in one single process. In this case, copper was concentrated in Stream 1 and 2, and Aluminium was concentrated in Stream 1 and 4. Different streams could go to different downstream processes depending on the strategy in industries. Therefore, the MDS presents as an effective method to purify the plastic fraction as well as to recover more metals in cable recycling.

 doi:10.20944/preprints202403.1063.v1

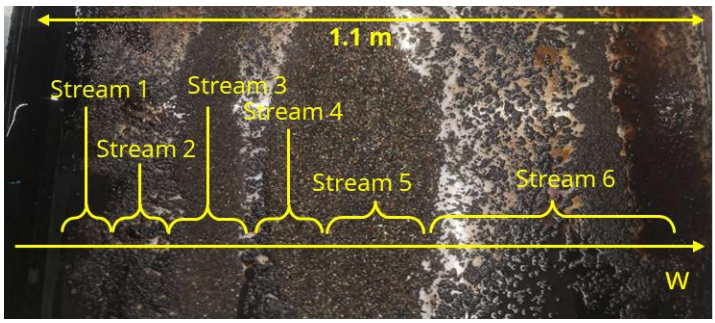

Figure 6. Top view of deposited wire scraps.

Table 3. Mass of each particle stream and Cu and Al contents in each stream.

Particle stream	Mass (g)	Cu (wt%)	Al (wt%)	Cu + Al (wt%)
MDS feedstock	488.2	1.02	1.13	2.15
Stream 1	8.9	41.88	1.58	43.46
Stream 2	7.6	1.38	0.62	1.99
Stream 3	65.1	0.41	0.53	0.94
Stream 4	111.0	0.31	2.95	3.25
Stream 5	219.0	0.12	0.72	0.84
Stream 6	22.4	0.25	0.29	0.54
Float	54.2	0.40	0.11	0.51

3.3. A Pilot Scale Facility of the Innovative MDS

To industrialize the new MDS process, a pilot scale facility was fabricated as shown in Figure 7 and the design has been patented [35]. The separation basin is filled with ferrofluid and is where the MDS happens. The hopper and vibratory feeder are fixed aside the basin to drop particles in the basin. After dropping, the particles quickly deposit on the bottom in seconds. The inclined permanent magnet as used in previous sections is placed underneath the basin. Note that the higher side of the magnet is on the feeder side and the lower side is on the front side of the figure. A mesh belt is continuously moving to transport deposited particles away from the basin. In the basin, belt lies on the horizontal bottom. The left side of the basin is a slope, where the belt climbs to take the particles out of the fluid. Note that the w axis which aligns in the width direction of the belt corresponds to the w axis in Figure 2 to Figure 6. On the collection side of the belt, particles can be collected as several separated streams along the w axis. The above design allows continuous production rather than batch processes as in the experiments, thus is applicable in industries.

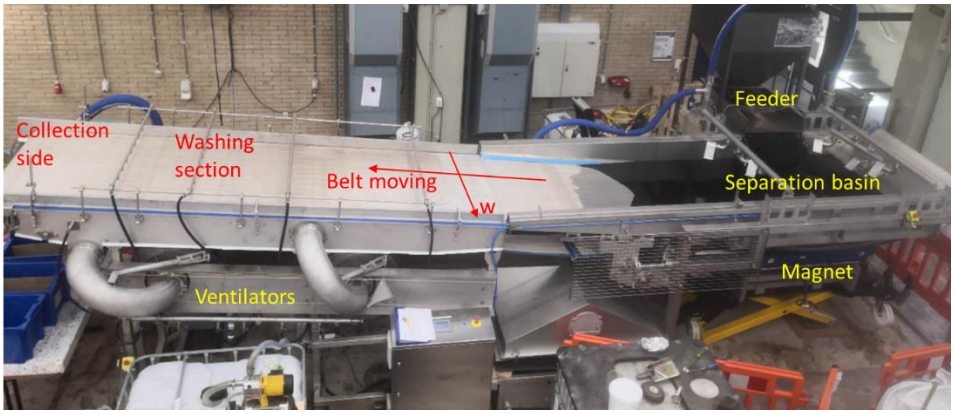

Figure 7. Pilot scale facility of the innovative MDS.

 doi:10.20944/preprints202403.1063.v1

The facility also has an important fluid recycling system to reduce the consumption of ferrofluid. The purpose is to retrieve the fluid taken out of the basin by the belt and particles and feed it back to the basin. In the washing section, water is sprayed on the belt and particles on it. The ventilators create a negative air pressure below the belt, thus the diluted ferrofluid can be sucked through the mesh belt and collected. The diluted fluid will be concentrated again to reach the required magnetization by some methods such as nano filtration, then it will be fed back to the separation basin to compensate for the consumption. Although it is not the case in Figure 5, the fluid recycling process is suggested to be continuous and automatic. The same facility is being optimized by TU Delft and the metal recycling company Myne in the Netherlands and is going to be used at industrial scale to sort various solid wastes such as cables, incinerator bottom ash and metal scraps for the concentration and purification of valuable metals and other materials.

4. Conclusions

An innovative MDS process has been developed for granular material sorting which has advantages over the existing industrialized MDS. The process applies an inclined planar magnet, a static magnetic fluid, and a basin with a horizontal bottom and without splitters. The process intrinsically avoids the negative effects of fluid turbulence and particle jamming. A particle sliding phenomenon was identified as a feature of the process which could help the separation. Experiments demonstrated the effectiveness of the MDS in the sorting of shredded PCBAs to concentrate valuable metals and the sorting of shredded electrical wires to purify the plastic fractions. A pilot scale facility based on the process has been introduced, where a belt conveying system allows a continuous production and a fluid recycling system reduces the consumption of ferrofluid.

5. Patents

The synthesis method of the ferrofluid used in this work has been patented [22,23].

The design of the planar magnet used in this work has been patented [21].

The design of the industrial facility based on the innovative MDS process introduced in this work has been patented [35].

Author Contributions: Conceptualization, P.R.; methodology, L.W. and P.R.; software, L.W.; validation, L.W. and P.R.; formal analysis, L.W.; investigation, L.W., M.V.B. and G.T.; resources, P.R. and F.D.M.; data curation, L.W.; writing—original draft preparation, L.W.; writing—review and editing, L.W., F.D.M., M.V.B. and G.T.; visualization, L.W.; supervision, P.R. and F.D.M.; project administration, P.R. and F.D.M.; funding acquisition, P.R. and F.D.M. All authors have read and agreed to the published version of the manuscript.

Funding: This research was funded by the European Union's Horizon 2020 research and innovation programme, grant number 958302 (PEACOC project). The APC was funded by TU Delft Library.

Data Availability Statement: Data available on request due to restrictions (e.g., privacy, legal or ethical reasons).

Acknowledgments: The authors would like to express their deep appreciation to Umincorp and Myne in the Netherlands and TREEE in Italy for providing the materials used in this work.

Conflicts of Interest: The authors declare no conflicts of interest.

References

1. Papell, S.S. Low viscosity magnetic fluid obtained by the colloidal suspension of magnetic particles. 1965.
2. Scherer, C.; Figueiredo Neto, A.M. Ferrofluids: properties and applications. *Brazilian journal of physics* **2005**, *35*, 718-727.
3. Rosensweig, R.E. Fluidmagnetic buoyancy. *Aiaa Journal* **1966**, *4*, 1751-1758.
4. Svoboda, J.; Fujita, T. Recent developments in magnetic methods of material separation. *Minerals Engineering* **2003**, *16*, 785-792.
5. Shimoiizaka, J.; Nakatsuka, K.; Fujita, T.; Kounosu, A. Sink-float separators using permanent magnets and water based magnetic fluid. *IEEE Transactions on Magnetics* **1980**, *16*, 368-371.
6. Odenbach, S. Ferrofluids-magnetisable liquids and their application in density separation. *Magnetic and Electrical Separation* **1970**, *9*, 1-25.

7. Mir, L.; Simard, C.; Grana, D. Recovery of nonferrous metals from scrap automobiles by magnetic fluid levitation. In Proceedings of the 3rd Urban Technology Conference and Technical Display, 1973; p. 959.
8. Muchova, L.; Bakker, E.; Rem, P. Precious metals in municipal solid waste incineration bottom ash. *Water, Air, & Soil Pollution: Focus* **2009**, *9*, 107-116.
9. Khalafalla, S.E.; Reimers, G.W. Separating nonferrous metals in incinerator residue using magnetic fluids. *Separation Science* **1973**, *8*, 161-178.
10. Hu, B.; Giacometti, L.; Di Maio, F.; Rem, P.C. Recycling of WEEE by magnetic density separation. In Proceedings of the The Sixth International Conference on Waste Management and Technology, 2011.
11. Bakker, E.J.; Rem, P.C.; Fraunholcz, N. Upgrading mixed polyolefin waste with magnetic density separation. *Waste Management* **2009**, *29*, 1712-1717.
12. Luciani, V.; Bonifazi, G.; Rem, P.; Serranti, S. Upgrading of PVC rich wastes by magnetic density separation and hyperspectral imaging quality control. *Waste management* **2015**, *45*, 118-125.
13. Serranti, S.; Luciani, V.; Bonifazi, G.; Hu, B.; Rem, P.C. An innovative recycling process to obtain pure polyethylene and polypropylene from household waste. *Waste management* **2015**, *35*, 12-20.
14. Hu, B. Magnetic density separation of polyolefin wastes. PhD thesis. Delft University of Technology, 2014.
15. Fujita, T.; Mori, S.; Mamiya, M.; Shimoiizaka, J. An improved sink-float testing apparatus for coal preparation using water based magnetic fluid. In Proceedings of the The 11th International Coal Preparation Congress, 1990; pp. 109-114.
16. Murariu, V.; Svoboda, J.; Sergeant, P. The modelling of the separation process in a ferrohydrostatic separator. *Minerals Engineering* **2005**, *18*, 449-457.
17. Weijmans, F.; Bakker, E.; Rem, P. Magnetic density separation of diamonds from gangue. *Environmental Engineering & Management Journal (EEMJ)* **2009**, *8*, 981.
18. Svobada, J. Separation in magnetic fluids: time to meet the technological needs. In Proceedings of the MINPREX 2000 Congress, 2000.
19. De Koning, J.R.A.; Bakker, E.J.; Rem, P.C. Sorting of vegetable seeds by magnetic density separation in comparison with liquid density separation. *Seed Science and Technology* **2011**, *39*, 593-603.
20. Bakker, E.J.; Rem, P.; Berkhout, A.J.; Hartmann, L. Turning magnetic density separation into green business using the cyclic innovation model. *The Open Waste Management Journal* **2010**, *3*, 99-116.
21. Polinder, H.; Rem, P.C. Magnet and device for magnetic density separation. WO2014158016A1, 2017.
22. Glazer, P.J.; Penners, R.A.; Berkhout, S.P.M.; Rem, P.C. Stock solution. US2022/0351886A1, 2022.
23. Glazer, P.J.; Paida, S.R.; Rem, P.C. Ferrofluid. US2022/0351887A1, 2022.
24. Rem, P.; Di Maio, F.; Hu, B.; Houzeaux, G.; Baltes, L.; Tierean, M. Magnetic fluid equipment for sorting secondary polyolefins from waste. *Environ. Eng. Manag. J* **2013**, *12*, 951-958.
25. Rem, P.C.; Berkhout, S.P.M. Magnetic density separation device and method. US10974255B2, 2021.
26. Thijs, L.C.; Kuerten, J.G.M.; Zeegers, J.C.H.; Tajfirooz, S. Magnetic density separation of particles in honeycomb-generated wake turbulence. *Chemical Engineering Science* **2023**, *278*, 118930.
27. Dellaert, R.A. Turbulence and particle behavior in a magnetic density separation application. PhD thesis. Eindhoven University of Technology, 2021.
28. Houzeaux, G.; Samaniego, C.; Calmet, H.; Aubry, R.; Vázquez, M.; Rem, P. Simulation of magnetic fluid applied to plastic sorting. *The Open Waste Management Journal* **2010**, *3*, 127-138.
29. Kloss, C.; Goniva, C.; Hager, A.; Amberger, S.; Pirker, S. Models, algorithms and validation for opensource DEM and CFD–DEM. *Progress in Computational Fluid Dynamics, an International Journal* **2012**, *12*, 140-152.
30. Kosse, J.J.; Dhallé, M.; Rem, P.C.; ter Brake, H.J.M.; ten Kate, H.H.J. Fundamental electromagnetic configuration for generating one-directional magnetic field gradients. *IEEE transactions on magnetics* **2021**, *57*, 1-10.
31. Kosse, J.J.; Dhallé, M.; Tomás, G.; Rem, P.C.; ter Brake, H.J.M.; ten Kate, H.H.J. Optimum coil-system layout for magnet-driven superconducting magnetic density separation. *IEEE transactions on magnetics* **2021**, *57*, 1-9.
32. Ning, C.; Lin, C.S.K.; Hui, D.C.W.; McKay, G. Waste printed circuit board (PCB) recycling techniques. *Chemistry and Chemical Technologies in Waste Valorization* **2018**, 21-56.
33. Díaz, S.; Ortega, Z.; McCourt, M.; Kearns, M.P.; Benítez, A.N. Recycling of polymeric fraction of cable waste by rotational moulding. *Waste Management* **2018**, *76*, 199-206.
34. de Araújo, M.C.P.B.; Chaves, A.P.; Espinosa, D.C.R.; Tenório, J.A.S. Electronic scraps–Recovering of valuable materials from parallel wire cables. *Waste management* **2008**, *28*, 2177-2182.
35. Di Maio, F.; Rem, P.C. Method of separating scrap particles, and particle separation assembly (Separation of materials heavier than water). 2031882, 2023.

 doi:10.20944/preprints202403.1063.v1